Supporting Information

Regulation of the light absorption and charge kinetics of SmCo DSAs to achieve an efficient photocatalytic CO_2RR

Xueyi Chen[1], Lingling Ding[1], Luxia Shao[1], Haowen Zuo[1], Yueli Liu[1,3,4,*], Wen Chen[2,3,*]

[1] State Key Laboratory of Silicate Materials for Architectures, School of Materials Science and Engineering, Wuhan University of Technology, Wuhan, 430070, P. R. China.

[2] State Key Laboratory of Advanced Technology for Materials Synthesis and Processing, School of Materials Science and Engineering, Wuhan University of Technology, Wuhan, 430070, P. R. China

[3] Hubei Longzhong Laboratory, Wuhan University of Technology Xiangyang Demonstration Zone, Xiangyang, 441000, P. R. China.

[4] Shenzhen Research Institute of Wuhan University of Technology, Shenzhen, 51800, P.R. China

[*] Corresponding authors:

Prof. Yueli Liu, E-mail: lylliuwhut@whut.edu.cn

Prof. Wen Chen, E-mail: chenw@whut.edu.cn

Experimental Section

Materials

1,3,5-triformylphloroglucinol (Tp, ≥97%) and p-phenylenediamine (Pa-1, ≥99.9%) were purchased from Jilin Chinese Academy of Sciences-Yanshen Technology Co., Ltd. 1,3,5-mesitylene (≥99.5%), 1,4-dioxane (≥99.5%), and methanol (≥99.5%) were obtained from Aladdin. Acetic acid (≥99.5%) was obtained from the Sinopharm Chemical Reagent Co., Ltd. $Sm(NO_3)_3 \cdot 6H_2O$ (99%), $Co(NO_3)_2 \cdot 6H_2O$ (99%) and bis-tris propane (btp) were obtained from Aladdin. All reagents were of analytical grade and used without further purification.

Synthesis of TpPa-1 COFs

TpPa-1 COFs was prepared by a simple solvothermal method with minor modifications[39]. Briefly, Tp (63 mg) and Pa-1 (48 mg) were dissolved in a mixture solution of 1,3,5-mesitylene and 1,4-dioxane (15 mL) in a ratio of 1:1. Then 1.5 mL of aqueous acetic acid (8 M) was added dropwise as a catalyst, and the mixture was sonicated for 20 min. The solution was reacted without stirring at 120℃ for 72 h under atmospheric pressure. Finally, a red solid was collected by centrifugation and washed with acetone, N,N-dimethylacetamide, and tetrahydrofuran for several times, and dried in vacuum oven at 80 ℃ for 24 h.

Synthesis of SmCo-btp/TpPa-1

In this research, $Sm(NO_3)_3 \cdot 6H_2O$ and $Co(NO_3)_2 \cdot 6H_2O$ were utilized as metal precursors, while btp was acted as the ligand to synthesize SmCo-btp/TpPa-1 catalyst.

SmCo-btp: Specifically, $Sm(NO_3)_3 \cdot 6H_2O$ (0.05 mmol), $Co(NO_3)_2 \cdot 6H_2O$ (0.1 mmol)

and btp (0.05 mmol) were dissolved in methanol (10 mL) to form a homogeneous solution, which was refluxed by condensation for 40 min under N_2 atmosphere. The gray sample was washed with methanol for several times, and dried in vacuum at 50 ℃ for overnight to obtain SmCo-btp.

SmCo-btp/TpPa-1: The above mentioned SmCo-btp (5 mg) was sonically dispersed in methanol (1 mL), while TpPa-1 COFs (45 mg) was similarly sonically dispersed in methanol (10 mL). Following complete dispersion, the two solutions were mixed and transferred into a three necked flask, and then refluxed for 12 h under N_2 atmospheres. After completion, the system was naturally cooled to room temperature, followed by washing with methanol and deionized water. Finally, the SmCo-btp/TpPa-1 was obtained by drying in vacuum oven at 50 ℃ for overnight.

Characterization

Powder X-ray diffraction (PXRD, MiniFlex600, Rigaku, Japan) was used to detect the crystal structure at room temperature using a diffractometer with Cu K α radiation in the 2θ range from 2 to 50°. The Fourier transformation infrared (FTIR) spectra were acquired in the 4000-400 cm^{-1} using a Nicolet 6700 spectrometer. X-ray photoelectron spectroscopy (XPS) measurements were performed on a Thermo ESCALAB 250 spectrometer. The position of the C 1s line at 284.8 eV was utilized to correct all XPS spectra. The microscopic morphology and structure of the samples were examined using field emission transmission electron microscope (FETEM, JEM-2100F, JEOL, Japan) and an aberration-corrected high-angle annular dark-field scanning transmission electron microscopy (HAADF-STEM, Titan Cube Themis G2 300),

respectively. The ultraviolet-visible diffuse reflectance spectra (UV-Vis DRS) were recorded on a UV-vis spectrophotometer (Shimadzu, UV-2700i, Japan). The position of conduction band of the samples was determined by measuring ultraviolet photo-electron spectra (UPS, ESCALAB 250Xi, Thermo Fisher Scientific, USA). The photogenerated charge carrier separation and lifetime of the samples were recorded using steady-state photoluminescence (PL) spectra (LabRam HR, HORIBA Jobin Yvon, France). Time-resolved photoluminescence (TRPL) spectra were recorded on a fluorescence lifetime spectro-photometer (Spirit 1040-8-SHG, Newport, USA) at an excitation wavelength of 365 nm. In-situ DRIFTS spectra were collected using an FTIR spectrometer (Nicolet iS50, Thermo Scientific, USA) equipped with a mercury cadmium telluride (MCT) detector.

Electrochemical Measurements

All of the electrochemical measurements were performed on a CHI-660e workstation (Shanghai Chenhua Instruments Co.), while Pt wire, Ag/AgCl (saturated KCl) and 0.01 M tetrabutylammonium hexafluorophosphate solution dissolved in acetonitrile were used as the counter electrode, reference electrode and electrolyte, respectively. Electrochemical impedance spectroscopy (EIS) was measured over the frequencies ranging from 0.1 Hz to 100 kHz with an amplitude of 5 mV. Photocurrent-time (i-t) curves with an interval of 40 s on/off switching were recorded on measured with an applied voltage of 0.2 V vs. Ag/AgCl. Mott-Schottky curve was tested in different frequency 1000, 1500 and 2000 Hz, respectively.

Photocatalytic Activity Measurements

The photocatalytic activities of all the catalysts were carried out in an automatic online gas analysis system (Labsolar-6A, Beijing Perfectlight Technology Co., Ltd., China) combined with gas chromatography (GC-9790II, Zhejiang Fuli Analytical Instruments Co., Ltd.). An appropriate amount of photocatalyst was dispersed in the 80 mL solution of acetonitrile, H_2O and TEOA (3:1:1) in the quartz reactor. After completely evacuating the air inside the reactor using a vacuum pump, ~55 kPa of high-purity CO_2 (99.999%) was introduced to achieve the adsorption equilibrium. The temperature of the reaction system was maintained at 298 K, and then the reaction system was irradiated under a 300 W Xe lamp (PLS-CS300, Beijing Perfectlight Technology Co., Ltd., China) with λ>420 nm cutoff filter.

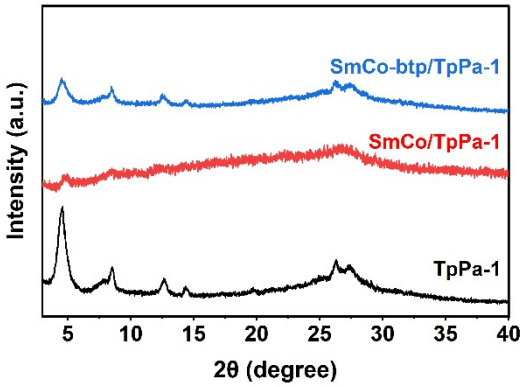

Fig. S1 PXRD patterns of TpPa-1, SmCo/TpPa-1 and SmCo-btp/TpPa-1.

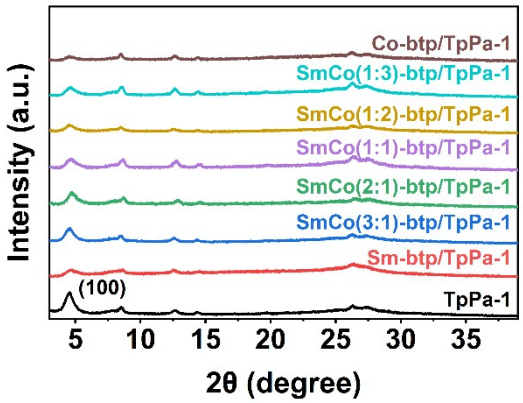

Fig. S2 PXRD patterns of SmCo-btp/TpPa-1 with different SmCo ratios.

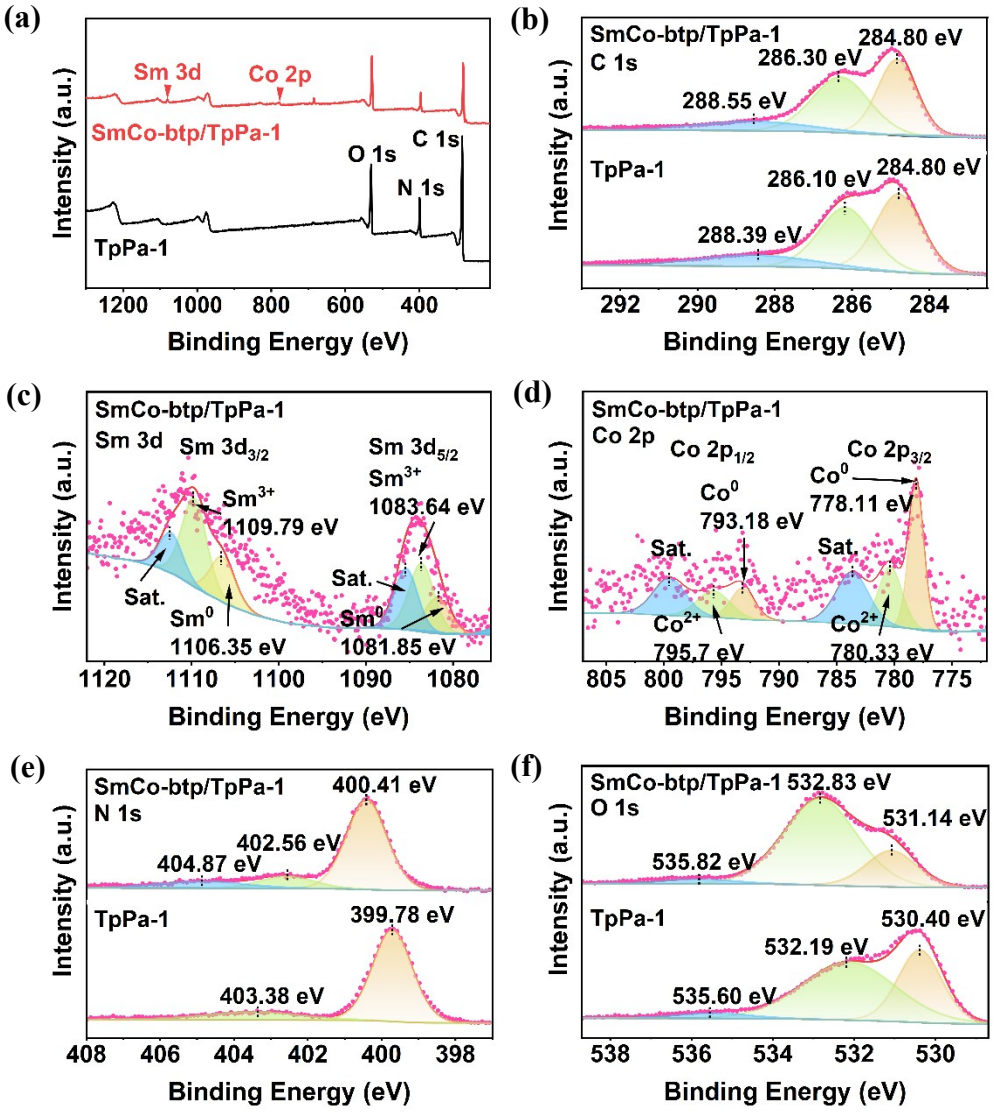

Fig. S3 XPS spectra of TpPa-1 COFs and SmCo-btp/TpPa-1: (a) Survey spectra, (b) C 1s, (c) Sm 3d, and (d) Co 2p, (e) N 1s, (f) O 1s.

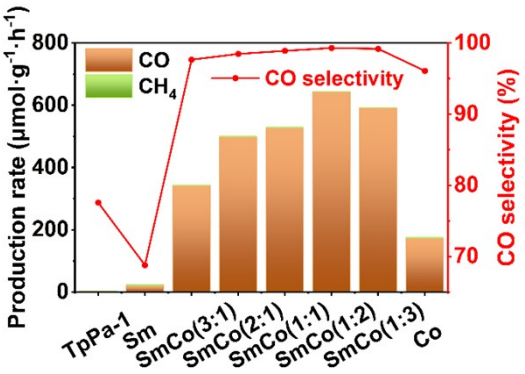

Fig. S4 Reduction production rate and selectivity of TpPa-1 and SmCo-btp/TpPa-1 with different SmCo ratios.

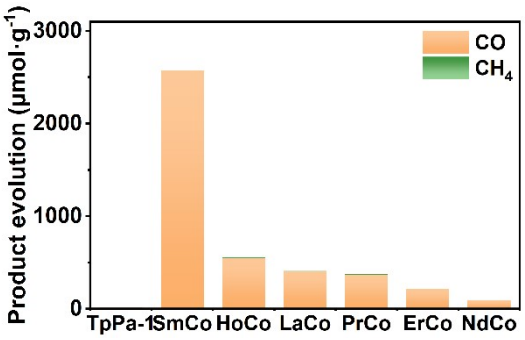

Fig. S5 Reduction production rate of TpPa-1 COFs and LnCo-btp/TpPa-1 (Ln = Sm, Ho, La, Pr, Er and Nd).

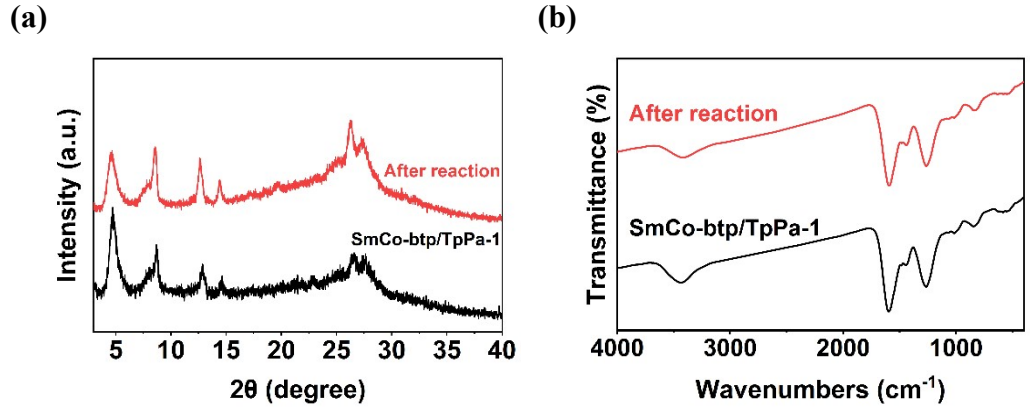

Fig. S6 (a) PXRD patterns and (b) FTIR spectra of SmCo-btp/TpPa-1 before and after photocatalytic cycle test.

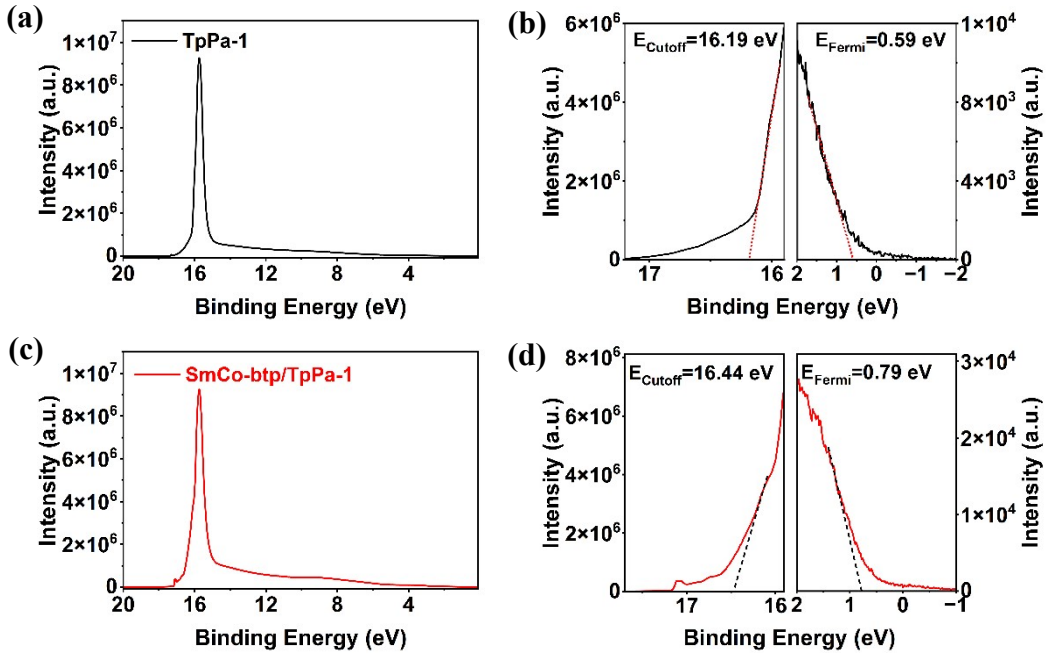

Fig. S7 Full scan UPS spectrc/TpPa-1.

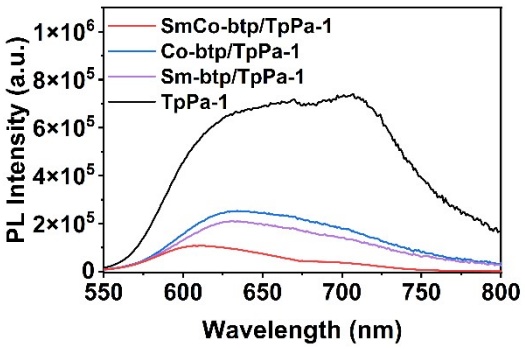

Fig. S8 steady-state PL spectrum of TpPa-1 COFs, Sm-btp/TpPa-1, Co-btp/TpPa-1, and SmCo-btp/TpPa-1.

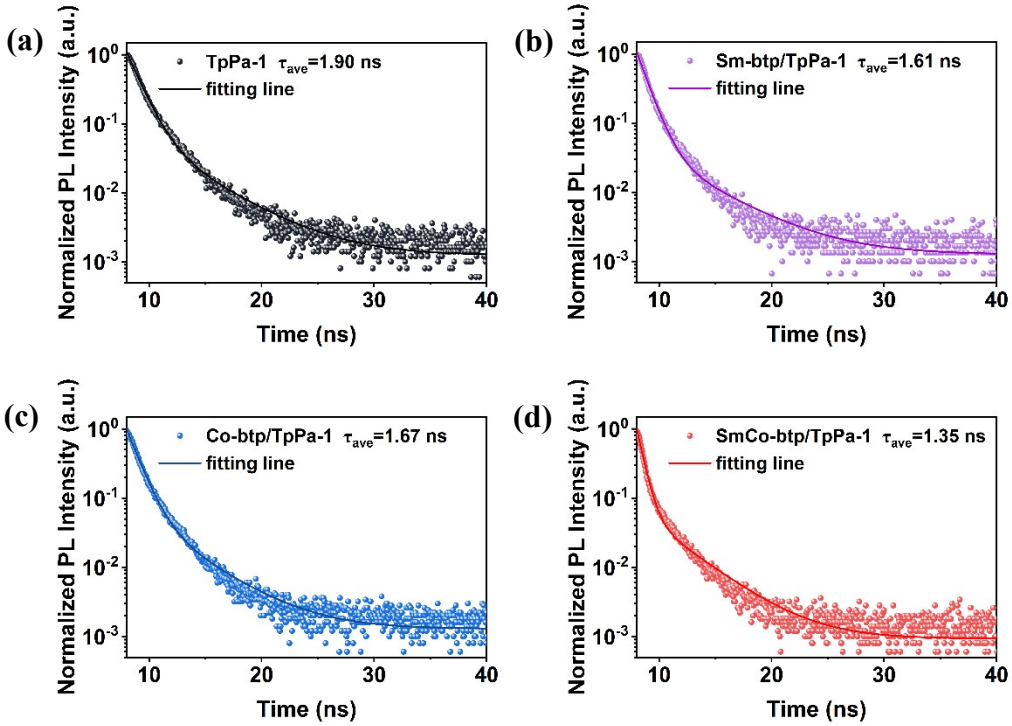

Fig. S9 TRPL spectrum of (a) TpPa-1 COFs, (b) Sm-btp/TpPa-1, (c) Co-btp/TpPa-1, and (d) SmCo-btp/TpPa-1.

Table S1 Photocatalytic CO_2 reduction performance of SmCo-btp/TpPa-1 with various SmCo metal ratios.

Catalyst	Production rates ($\mu mol \cdot g^{-1} \cdot h^{-1}$)		CO selectivity (%)
	CO	CH_4	
TpPa-1 COFs	4.15	0.30	77.57
Sm-btp/TpPa-1	21.95	2.49	68.79
SmCo(3:1)-btp/TpPa-1	341.99	2.06	97.65
SmCo(2:1)-btp/TpPa-1	498.34	1.96	98.45
SmCo(1:1)-btp/TpPa-1	528.36	1.50	98.88
SmCo(1:2)-btp/TpPa-1	643.36	1.15	99.29
SmCo(1:3)-btp/TpPa-1	590.62	1.24	99.17
Co-btp/TpPa-1	173.98	1.78	96.07

The overall metal loading remains constant, with only the proportional ratios of the two metals being adjusted.

Table S2 Comparison of photocatalytic CO_2 reduction performance of metal atoms catalyst.

Catalyst	CO yield ($\mu mol \cdot g^{-1} \cdot h^{-1}$)	CO selectively (%)	Solvent	Reference
SmCo-btp/TpPa-1	643.36	99.29	MeCN/H_2O/TEOA	This work
Co/TpPa-1	414.5	99.45	MeCN/H_2O/TEOA	1
CoRu-HCNp	27.31	/	H_2O	2
COF-5/CoAl-LDH	53.08	94.6	MeCN/H_2O	3
PcCo/Zn-Salen-COF	138.4	/	H_2O	4
COF-RuBpy-Co	547	75	MeCN/TEOA/BIH	5
Mn_1Co_1/CN	47	100	H_2O	6
$BTOCu_2Ru_{0.5}$	180.67	/	MeCN/H_2O	7
TCOF-MnMo6	37.25	100	H_2O	8
Co_1Ag_1−PCN	11.71	70.1	MeCN/H_2O	9
CdS@COF-ZnCo	507.13	72	MeCN/H_2O/BIH	10
In-suit Zn/TpBpy	281.75	99.96	MeCN/H_2O/TEOA	11
Au@CN/Auc/G	61.75	83	H_2O/TEOA	12
In-NTO	6.34	95.9	H_2O	13

Table S3 The fitted TRPL parameters of TpPa-1 COFs, Sm-btp/TpPa-1, Co-btp/TpPa-1, and SmCo-btp/TpPa-1.

Sample	τ_1 (ns)	A_1	τ_2 (ns)	A_2	τ_{ave} (ns)
TpPa-1 COFs	0.94	1.11	0.08	4.31	1.90
Sm-btp/TpPa-1	1.06	0.92	0.05	4.55	1.61
Co-btp/TpPa-1	0.90	1.00	0.07	3.90	1.67
SmCo-btp/TpPa-1	1.06	0.55	0.06	3.55	1.35

References

1. Liu, Y.; Shao, L.; Ding, L.; Chen, X.; Bao, Y.; Chen, W. In situ anchoring of Co single atoms within keto-enamine COFs via the coordination of an interlayer N atom with Co for the enhanced photocatalytic CO_2 reduction efficiency. *ACS Appl. Mater. Interfaces* **2025**, 17(18), 26722-26730.
2. Cheng, L.; Yue, X.; Wang, L.; Zhang, D.; Zhang, P.; Fan, J.; Xiang, Q. Dual-single-atom tailoring with bifunctional integration for high-performance CO_2 photoreduction. *Adv. Mater.* **2021**, 33(49), 2105135.
3. Ou, S.; Zhou, M.; Chen, W.; Zhang, Y.; Liu, Y. COF-5/CoAl-LDH nanocomposite heterojunction for enhanced visible-light-driven CO_2 reduction. *ChemSusChem* **2022**, 15(7), e202200184.
4. Dong, H.; Wang, Y.; Fang, L.; Wu, D.; Bai, L.-W.; Jiang, Y.; Chu, X.; Zhang, H.-Y.; Yang, Y.; Zhang, F.-M. Design synergistic dual metal sites in Z-scheme system of metal phthalocyanine and metal-covalent organic framework for photocatalytic diluted CO_2 reduction. *Nano Energy* **2025**, 143, 111305.
5. Gong, L.; Liu, L.; Zhao, S.; Yang, S.; Si, D.; Wu, Q.; Wu, Q.; Huang, Y.; Cao, R. Rapid charge transfer in covalent organic framework via through-bond for enhanced photocatalytic CO_2 reduction. *Chem. Eng. J.* **2023**, 458, 141360.
6. Ou, H.; Ning, S.; Zhu, P.; Chen, S.; Han, A.; Kang, Q.; Hu, Z.; Ye, J.; Wang, D.; Li, Y. Carbon nitride photocatalysts with integrated oxidation and reduction atomic active centers for improved CO_2 conversion. *Angew. Chem. Int. Ed.* **2022**, 61(34), e202206579.

7. Liu, L.; Hu, J.; Sheng, Y.; Akhoundzadeh, H.; Tu, W.; Siow, W. J. S.; Ong, J. H.; Huang, H.; Xu, R. Ru single atom dispersed Cu nanoparticle with dual sites enables outstanding photocatalytic CO_2 reduction. *ACS Nano* **2024**, 18(38), 26271-26280.
8. Lu, M.; Zhang, M.; Liu, J.; Yu, T.; Chang, J.; Shang, L.; Li, S.; Lan, Y. Confining and highly dispersing single polyoxometalate clusters in covalent organic frameworks by covalent linkages for CO_2 photoreduction. *J. Am. Chem. Soc* **2022**, 144(4), 1861-1871.
9. Deng, A.; Zhao, E.; Li, Q.; Sun, Y.; Liu, Y.; Yang, S.; He, H.; Xu, Y.; Zhao, W.; Song, H.; Xu, Z.; Chen, Z. Atomic cobalt-silver dual-metal sites confined on carbon nitride with synergistic Ag nanoparticles for enhanced CO_2 photoreduction. *ACS Nano* **2023**, 17(12), 11869-11881.
10. Zou, L.; Sa, R.; Zhong, H.; Lv, H.; Wang, X.; Wang, R. Photoelectron transfer mediated by the interfacial electron effects for boosting visible-light-driven CO_2 reduction. *ACS Catal.* **2022**, 12(6), 3550-3557.
11. Zhou, M.; Ding, L.; Chen, K.; Bao, Y.; Liu, Y.; Chen, W. Designing Zn atomic coordination sites within TpBpy COFs for efficient photocatalytic CO_2 reduction under visible light irradiation. *Chem. Eng. J.* **2025**, 516, 164339.
12. Ziarati, A.; Zhao, J.; Afshani, J.; Kazan, R.; Mellor, A. P.; Rosspeintner, A.; McKeown, S.; Bürgi, T. Advanced catalyst for CO_2 photo-reduction: From controllable product selectivity by architecture engineering to improving charge transfer using stabilized Au clusters. *Small* **2023**, 19, 2207857.

13. Tian, F.; Li, Y.; Yan, X.; Zhu, H.; Liang, J.; Zhang, H.; Han, N. Asymmetric-coordinated indium single atoms for highly selective photocatalytic CO_2 reduction. *Carbon Energy* **2026**, e70166.